AIAA SciTech Forum
7-11 January 2019, San Diego, California
AIAA Scitech 2019 Forum

10.2514/6.2019-2157

A Study of the Aerodynamics of a Low Reynolds Number Airfoil Translating Across a Uniform-Shear Approach Flow

Mitchell B. Albrecht,* Ahmed M. Naguib,† and Manoochehr M. Koochesfahani‡
Michigan State University, East Lansing, Michigan, 48824

This work investigates the aerodynamics of a NACA-0012 airfoil moving at steady velocity and fixed geometric angle of attack across a uniform-shear flow at low chord Reynolds numbers. The airfoil translates across a uniform-positive-shear approach flow, with non-dimensional shear rate values ranging 0.40-0.66 and chord Reynolds numbers ranging 1.00×10^4-1.61×10^4, where the ratio of the airfoil velocity relative to the approach stream velocity ranges 0.040-0.066. Airfoils performing similar dynamic motion in uniform flow may be analyzed in a Galilean reference frame; however, no equivalent analysis exists for uniform-shear flows. The current results for an airfoil moving at steady velocity across a shear flow in a Galilean frame of reference show the lift coefficient, obtained by direct measurement, may be approximated by the lift coefficient on a stationary airfoil under the same flow conditions at negative and low-positive angles of attack. However, an asymmetry is observed where a significant difference occurs between the moving and the stationary airfoils at positive angles of attack approaching stall. This difference is associated with a change in the airfoil stall behavior due to movement across the shear zone.

I. Introduction

Much of the research on unsteady (pitching, plunging, or both simultaneously) airfoil aerodynamics has focused on uniform freestream approach conditions. This leaves studies of unsteady airfoils in non-uniform-velocity approach (shear) flows practically unexplored. Only recently are studies beginning to uncover the effects of shear on airfoils. One study on a stationary airfoil in the presence of viscous positive uniform-shear uncovered a phenomenon in which negative lift occurs at zero angle of attack (AoA) [1], opposite of inviscid theory [2], and becomes increasingly negative with increasing non-dimensional shear rate. A second study investigated a harmonically-pitching airfoil in the presence of positive uniform shear, noting considerable differences in the wake and the average lift characteristics compared to uniform flow [3]. These recent developments on the effects of shear on both steady and unsteady airfoils demonstrate a lack of understanding of airfoils in shear in general. Despite the lack of knowledge of unsteady airfoils in shear, these conditions are common, for example, during aircraft takeoff and landing where shear flows, such as atmospheric wind gradients and wakes behind structures, are pervasive. Thus, there is a need to understand the fundamental aerodynamics of airfoils in the presence of the coupled complexities of freestream shear and airfoil motion.

Experiments are carried out in the present study where a NACA-0012 airfoil traverses steadily across a canonical uniform-shear approach flow (i.e. where the freestream velocity varies linearly in the cross-stream direction) in a water tunnel, with reference coordinates (X, Y) along the water tunnel centerline. Figure 1 illustrates this problem, where the airfoil of chord c, at a geometric angle of attack α, experiences an approach stream with reference streamwise velocity u_0 at its quarter-chord a distance Y_a from the water tunnel centerline. The airfoil translates with a steady velocity $V_a = dY_a/dt$ across a positive uniform-shear flow characterized by a freestream velocity $u_\infty(Y)$, where the flow varies linearly between regions of high- and low-speed uniform flow (u_1 and u_2, respectively), creating a shear zone of thickness δ and non-dimensional shear rate K (see Fig. 1 for definition). As the airfoil translates across this three-segment velocity profile in time t, u_0 changes as $u_0 \equiv u_\infty(Y_a(t))$, which changes the non-dimensional shear rate correspondingly. This unsteady nature of the problem, despite steady freestream and airfoil motion, may be characterized by the non-dimensional rate of change of u_0; specifically:

$$\frac{du_0}{dt}\frac{c}{u_0^2} \tag{1}$$

* Graduate Student, Mechanical Engineering, 1449 Engineering Research Ct A108, East Lansing, MI 48824, AIAA Member.
† Professor, Mechanical Engineering, 1449 Engineering Research Ct C128, East Lansing, MI 48824, AIAA Associate Fellow.
‡ Professor, Mechanical Engineering, 1449 Engineering Research Ct A131, East Lansing, MI 48824, AIAA Associate Fellow.

This unsteadiness may be rewritten in terms of the local ratio of airfoil velocity to freestream velocity V_r and the non-dimensional shear rate by

$$\frac{du_0}{dt}\frac{c}{u_0^2} = \frac{du_\infty}{dY_a}\frac{dY_a}{dt}\frac{c}{u_0^2} = \frac{du_\infty}{dY_a}\frac{V_a c}{u_0^2} = \frac{V_a}{u_0} \times \frac{du_\infty}{dY_a}\frac{c}{u_0} = V_r \times K \tag{2}$$

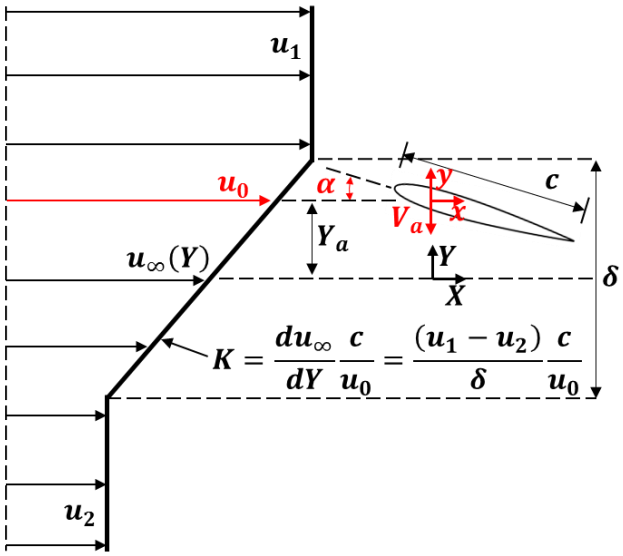

Fig. 1 Uniform-shear flow and translating airfoil configuration in which the airfoil translates at geometric angle of attack α and steady velocity V_a from the high- to the low-speed uniform regions of the flow.

Compared to uniform flow, the movement of an airfoil across a non-uniform-velocity approach flow introduces further complexity by making common aerodynamic definitions unclear. For a uniform-velocity freestream, the steady cross-stream movement of the airfoil in the laboratory frame of reference results in an effective AoA and freestream velocity that are different from those of the stationary airfoil. The modified AoA and freestream velocity are those observed in a Galilean frame of reference moving with the airfoil. The effective AoA α_{eff} is calculated from α and V_r, where α_i is the induced angle of attack due to airfoil motion:

$$\alpha_i = \tan^{-1}\left(\frac{V_a}{u_0}\right) = \tan^{-1}(V_r) \tag{3}$$

$$\alpha_{eff} = \alpha + \alpha_i \tag{4}$$

When shear is present in the freestream, a fundamental difficulty arises where α_{eff} cannot be defined uniquely since the freestream velocity varies across the approach stream. In this study, u_o is used to compute α_{eff}, leaving the issue of non-uniqueness of this choice to be addressed in future work. It should be noted that since u_o varies with the airfoil position in the shear flow, both u_0 and α_{eff} become functions of time, and hence the flow is unsteady even in the Galilean frame. Figure 2 provides a graphical representation of all the terms in Eqs. (3) and (4) in a Galilean frame of reference compared to the laboratory reference frame. The figure also depicts the laboratory (x, y) and the Galilean (x', y') frames of reference, in which the latter is obtained by rotating the former through α_i. Similarly, the drag and the lift forces in the Galilean frame of reference (D' and L', respectively) are obtained by the same rotation applied to the drag and the lift forces in the laboratory frame of reference (D and L, respectively). The corresponding local effective approach velocity magnitude in the Galilean frame is

$$u_{eff} = \sqrt{u_0^2 + V_a^2} = u_0\sqrt{1 + V_r^2} \tag{5}$$

which allows for the calculation of the lift coefficient in the Galilean frame of reference for the airfoil of span b in a fluid of density ρ:

$$C_L = \frac{L'}{\frac{1}{2}\rho u_{eff}^2 cb} \tag{6}$$

Both reference frames are the same at the limit of $V_a = 0$, meaning $\alpha = \alpha_{eff}$ and $u_0 = u_{eff}$ for a stationary airfoil. For simplicity and consistency, results reported herein use α_{eff} and C_L for both the stationary and the moving airfoils.

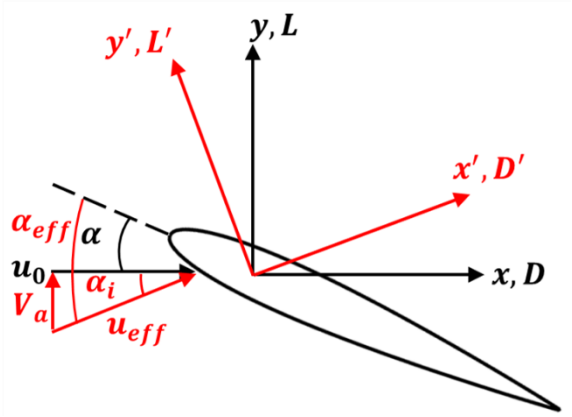

Fig. 2 Graphical comparison of the laboratory (black) and Galilean (red) reference frames. The Galilean reference frame is obtained by rotating the laboratory reference frame through α_i.

The present work has several objectives. First is to establish and verify the accuracy of an experimental setup used to study the aerodynamics of airfoils traversing across a substantial fraction of the test section of a water tunnel. Second is to use a load cell to measure the lift history acting on a NACA-0012 airfoil as it traverses across a uniform-shear stream at different angles of attack. Third is to compare the force on the moving airfoil to that of a stationary airfoil inside the shear zone. The motivation of this comparison is to investigate if, as is the case for uniform freestream, the forces acting on the moving airfoil in a Galilean frame are the same as those acting on a stationary airfoil after taking into account α_{eff} and u_{eff}. Since the former problem is unsteady and the latter is steady, a meaningful connection between the moving and stationary airfoils is expected to be possible only under quasi-steady conditions (i.e. when the flow dynamics caused by the airfoil movement across the shear is sufficiently slow for the flow to adapt to the changing position of the airfoil within the shear zone). Knowing whether a connection between the stationary and the moving airfoil aerodynamics exists, and the conditions under which such a connection works, has a useful, practical ramification. In particular, if such a connection is found, it alleviates the need to conduct experiments and/or computations on a moving model to study the aerodynamics of airfoils traversing across a shear zone. The present study is conducted at chord Reynolds number Re_c = 1.00×10^4-1.61×10^4, where, given kinematic viscosity of the fluid ν:

$$Re_c = \frac{u_{eff} c}{\nu} \tag{7}$$

A complimentary investigation in a wind tunnel [4] involves similar measurements at a higher Reynolds number Re_c ≈ 7.5×10^4, in order to investigate Reynolds number effects.

II. Experiments

A. Water Tunnel Experimental Setup

The experiments are conducted in a closed-return, free-surface water tunnel (Engineering Laboratory Design, ELD) at the Turbulent Mixing and Unsteady Aerodynamics Laboratory (TMUAL) at Michigan State University. The

tunnel has a test section of 61 cm × 61 cm × 244 cm, and is equipped with a three-degree-of-freedom (3DOF) servo motion system capable of producing pitch, plunge, and surge motions of airfoils (see Fig. 3). The present work utilizes only the pitch and plunge motors. A NACA-0012 airfoil with chord c = 12 cm and span b = 61cm (aspect ratio of 5.1) is mounted about its quarter-chord to the rotary servo motor with an ATI Mini40 six-component force and torque transducer along the connecting shaft. The Parker rotary servo motor (MPP1154A9D-KPSN) is mounted to the carriage of a Parker servo-controlled linear motor (T4DB0436NPAMA4). The rotary motor is fitted with a high-resolution encoder with pitch angle resolution of 0.003°, and the linear motor is fitted with a linear-magnetic encoder with linear position resolution of 1 μm. Two polycarbonate plates extend approximately 61 cm (5.1c) upstream and downstream of the airfoil shaft and span the width of the test section. The purpose of these plates is to maintain contact with the water surface to prevent disturbing the free surface during airfoil translation, and to provide a well-defined boundary condition. A 4.4 cm gap between the plates provides clearance for the motion of the plunging airfoil for a travel range up to 61 cm. The airfoil root and tip maintain clearance gaps of less than 0.75 mm (0.63% c) with the plates and the test-section bottom, respectively.

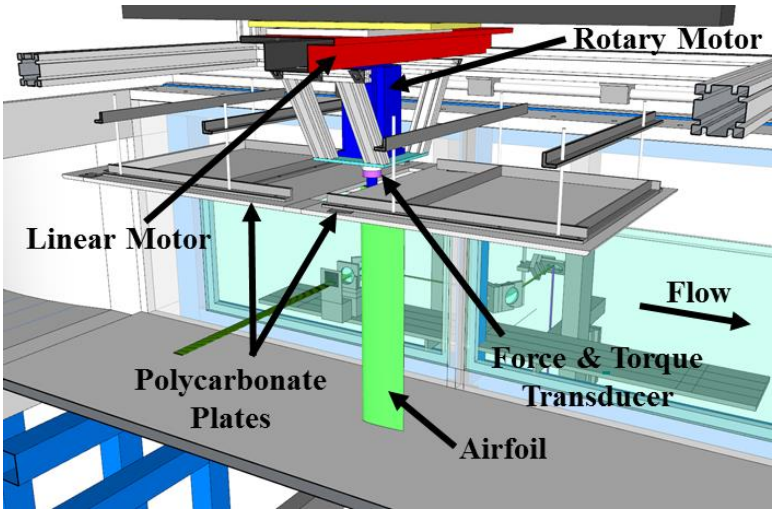

Fig. 3 Section view of a 3D model of the test section of the TMUAL water tunnel facility showing the airfoil, transducer, and motor system arrangement.

The tunnel is equipped with a 3DOF traversable optics bench capable of steering UV laser light into the tunnel for molecular tagging velocimetry (MTV) measurements (see Fig. 4). Molecular tagging velocimetry is a whole-field non-intrusive measurement technique that relies on a flowing medium premixed with molecules that can be turned into long-lifetime tracers upon excitation by photons of a particular wavelength [5, 6]. Typically, a pulsed laser is used to "tag" the regions of interest, and those tagged regions are interrogated at two successive times within the lifetime of the tracer. The measured displacement vector provides the estimate of the velocity vector. The present work employs MTV using a phosphorescent supramolecule tracer [5], excited by a COMPex Pro 205 XeCl 308 nm excimer laser. A series of mirrors and lenses direct the focused laser beam through a beam blocker that separates the beam into several individual lines for one-component MTV (1c-MTV). One-component MTV measures the Lagrangian displacement in the direction normal to the tagged line at every pixel along the line, providing one component of the flow velocity at very high spatial resolution. The line displacement is calculated using the spatial correlation techniques described in Ref. [7].

Force measurements are conducted for both cases of a stationary and a translating airfoil. In the former case, the pitch motor holds the airfoil AoA fixed while the plunge motor is off with its carriage mechanically locked in place. For the translating airfoil, the linear motor translates the airfoil across the approach stream while the pitch motor actively holds the airfoil AoA. Tests had shown that the coupled use of both motors does not negatively interfere with the moving airfoil measurements.

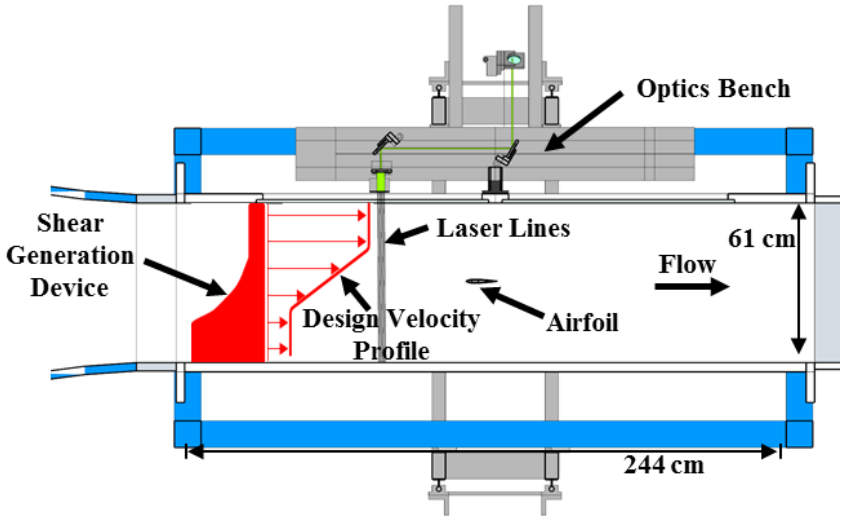

Fig. 4 Section view from the top of the test section of the water tunnel showing the shear generation device used to create a prescribed freestream velocity profile.

B. Shear Flow Generation and Characterization

A shaped honeycomb technique, developed in Ref. [8] and refined in Ref. [9], is used to generate a uniform-shear velocity profile in the freestream of the water tunnel based on the desired three-segment velocity profile. The honeycomb structure is placed at the test section entrance in the path of the freestream flow (see Fig. 4). Varying the streamwise length of the honeycomb along the cross-stream direction produces variable flow resistance, generating a non-uniform velocity profile. In the present work, a honeycomb with 3.175 mm-diameter cells is profiled to produce a linearly-varying-velocity zone, bounded by high- and low-speed uniform-velocity regions.

One-component MTV is used to measure the streamwise flow velocity of the approach stream in uniform and uniform-shear flows. To form image pairs for correlation, a continuous time series of images taken immediately after the laser pulse are averaged together to form a single "undelayed" image of an undisturbed molecularly-tagged line. A second, continuous time series of images are taken at time delays, in the range 7-8 ms, after the laser pulse to capture the displacement of the line of tagged molecules. These "delayed" images are each correlated with the average undelayed image to determine the displacement of every line in the time series. The location of the flow measurements is far enough upstream of the airfoil such that the presence of the airfoil does not influence the flow, and far enough downstream of the shear generation device that the flow is sufficiently developed. The images are captured using two PCO Pixelfly cameras mounted adjacently below the water tunnel, aimed vertically, such that the two frames overlap by roughly 3.5% in the cross-stream direction. The uniform flow measurements are recorded in these two frames at full frame resolution of 1392 pixels × 1040 pixels (cross-stream direction × streamwise direction), in the approximate region $-1.25 < Y/c < 1.25$, where $Y/c = 0$ is the water tunnel cross-stream centerline. The shear flow measurements are recorded in 4 total frames (two frames per position, two camera positions) with frame resolution of 696 pixels × 1040 pixels, in the approximate region $-2.2 < Y/c < 2.2$. This cross-stream domain is chosen to encompass not only the moving airfoil range, but to also measure the uniform flow regions of the three-segment profile. Based on correlating the individual undelayed images with their respective average image, the streamwise sub-pixel uncertainty is approximately 0.1 pixel (0.011 mm), which for the corresponding time delay range results in a velocity uncertainty of less than 1.6% for u_0 = 10 cm/s.

The measured uniform freestream profile indicates a mean velocity of 10 cm/s, with a spatial RMS of 4.9%. Based on water temperature measurements during data acquisition, the corresponding Re_c is 1.28×10^4. The design and the experimentally measured velocity profiles of the uniform-shear flow are given in Fig. 5. Compared with the design shear profile, the experimental shear profile exhibits an "undershoot" where the shear layer and the low-speed uniform region meet, and a high-speed zone that does not reach the design velocity magnitude. As shown in Fig. 6, the temporal RMS is generally around 2% of the reference velocity, except in the region associated with the undershoot where it spikes to around 3%. The design velocity profile is characterized by u_0 = 10 cm/s at the centerline and K = 0.5 in the shear region, whereas the experimental profile is characterized by u_0 = 10.1 cm/s at the centerline and K = 0.52 in the uniform-shear region. Based on temperature measurements of the water tunnel during data acquisition, the Reynolds number is 1.31×10^4. The uniform-shear region for the measured profile is defined as the part of the shear flow between

u_1 and u_2, excluding the undershoot region where the shear rate becomes non-uniform, as highlighted in Fig. 5. A linear least-squares fit of the velocity in the uniform-shear region determines the shear rate. The resulting thickness of this part of the shear layer is δ/c = 1.7, compared to the design profile's δ/c = 2.0.

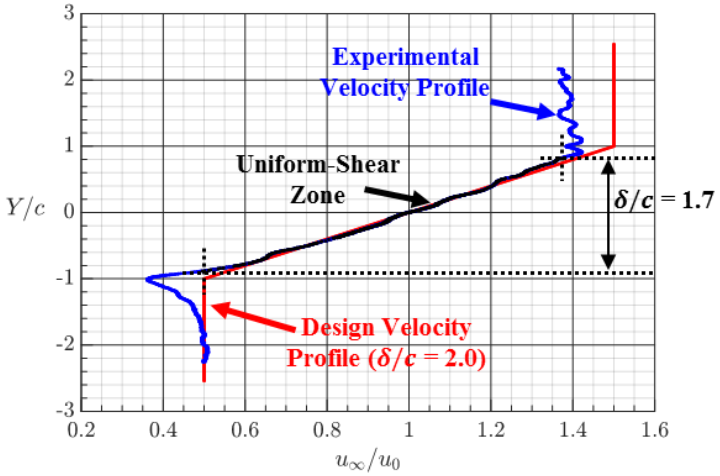

Fig. 5 Comparison of the design (red, u_0 = 10 cm/s) and the experimentally generated (blue, u_0 = 10.1 cm/s) velocity profiles for the shear generation device used in the present work. The uniform-shear region for the measured profile is given in black.

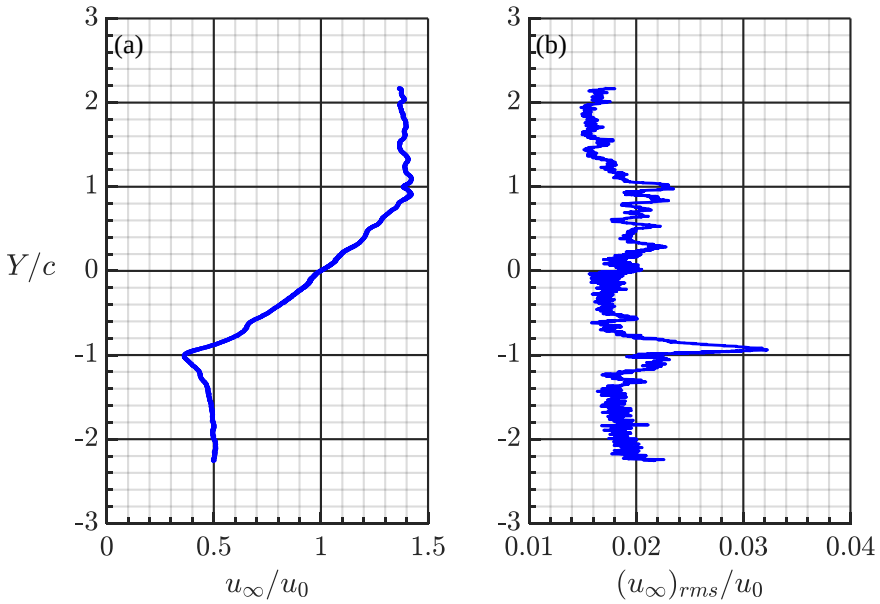

Fig. 6 Plots of the measured shear flow (a) mean velocity profile and (b) RMS velocity profile for Re_c = 1.31×10^4 with K = 0.52 based on u_0 = 10.1 cm/s on the tunnel centerline.

C. Lift Force Measurement Procedure

Lift force is measured using the six-axis ATI Mini40 load cell. The measurements are performed for both stationary and translating airfoils as well as with/without the presence of shear in the freestream over the range -15° < α_{eff} < 15°. The stationary airfoil measurements are used to establish a baseline against which to compare the moving airfoil, in both uniform and uniform-shear flows. For all measurements, to zero the load cell, force measurements are first recorded without flow and the resulting average is subtracted from subsequent "flow-on" force measurements. The

total time for measurements at a given AoA is set to be sufficiently long to ensure convergence of the mean force, yet short enough to minimize drift in the sensor's bias. Zero AoA is found by first setting the airfoil's chord to be parallel to the test section's sidewalls. The zero-lift AoA is then determined by fitting a line to the force measurements between ±3° AoA in uniform flow and determining the value where the measured lift crosses zero. The mean forces measured on the stationary airfoil are calculated from time-averaging 180 second-long ($u_\infty t/c$ = 150) time series. Uncertainty estimates are determined by defining each 10 second segment of data as an independent dataset and computing the standard deviation due to the variation in the mean lift computed from the different segments. The resulting uncertainty of lift force is less than 0.007 N, corresponding to C_L = 0.02 uncertainty for u_0 = 10 cm/s.

For the translating-airfoil experiments, the airfoil begins motion 18 cm (1.5c) above the water tunnel centerline, and plunges a distance of 36 cm (3c) at a velocity V_a = 5 mm/s before coming to rest 18 cm (1.5c) below the water tunnel centerline. The total motion stroke corresponds to 59% of the test section width. For the shear flow, the airfoil moves from the high-speed to the low-speed side of the shear layer. The plunge velocity ratio is 5% based on the tunnel centerline velocity, compared to 6% based on a typical 3.5° glideslope of a landing aircraft. Force data are recorded continuously during five sets of five individual plunges, with each set including flow-off measurements to zero the load cell. The measurement time of each set is less than 15 minutes for the bias drift to remain negligible. The total number of motion strokes is 25, which are then phase-averaged relative to the start of motion (as determined from the plunge motor's position encoder) to give the phase-averaged force as a function of cross-stream position and time. During motion, the airfoil tip oscillates at the airfoil structural frequency, and optical measurements of these oscillations had shown the amplitude to be less than 0.5% of the chord. To remove influence of these oscillations on the lift force history, the phase-averaged lift history is temporally averaged. The lift and the drag measurements are recorded in the laboratory frame of reference, which for the moving airfoil must be transformed into the Galilean frame of reference. As mentioned in Section II, this is achieved by simply applying a rotation matrix using α_i:

$$\begin{bmatrix} D' \\ L' \end{bmatrix} = \begin{bmatrix} \cos(\alpha_i) & -\sin(\alpha_i) \\ \sin(\alpha_i) & \cos(\alpha_i) \end{bmatrix} \begin{bmatrix} D \\ L \end{bmatrix} \tag{8}$$

This allows comparison of the force at a given position in the tunnel with the mean force measurement on the stationary airfoil at the same cross-stream position and effective AoA. Each plunge is considered as an independent dataset, resulting in an uncertainty estimate of lift force of less than 0.02 N (C_L of 0.055, based on the test section centerline velocity). For each cross-stream measurement position with which to compare the equivalent stationary airfoil result, the mean velocity profile is averaged over one airfoil thickness to reduce the influence of spatial variation of the approach flow. The lift force on the moving airfoil is averaged over the same range for consistency. For this work, the three cross-stream measurement positions investigated are: $Y_a/c = 0$ and $Y_a/c = \pm 0.5$.

III. Results and Discussion

A. Uniform Flow Results

In traditional force balance measurements, the test model is kept on the centerline of the test section while stationary, or oscillating over a stroke/amplitude that is negligible relative to the test section's width. Therefore, an important aspect of this study is to validate the present experimental approach and ensure that the relatively large motion of the airfoil does not cause significant measurement artifacts due to blockage/confinement effects. To do so, measurements of the C_L on the stationary and the moving airfoil are compared under uniform freestream conditions. In the comparison, variation in the stationary airfoil's time-averaged C_L with α is compared with the phase-averaged C_L variation with the α_{eff} for the moving airfoil at the time instant when the latter is located at the same cross-stream location as the former. The comparison was made at several cross-stream locations, encompassing the motion stroke used for the shear flow experiments. For the plunge velocity ratio of 5% used here, the results in Fig. 7 show that the stationary and the moving airfoil C_L-*vs.*-α_{eff} characteristics agree with each other for each of the cross-stream positions investigated. Blockage/confinement effects are shown to have a negligible impact on the stationary and moving airfoils at the cross-stream positions and the flow conditions investigated here. The agreement in the lift characteristics in the laboratory and the Galilean frames of reference under uniform freestream conditions demonstrates the viability of the present experimental approach for obtaining lift measurements when the airfoil is traversing across the shear flow over the measurement domain.

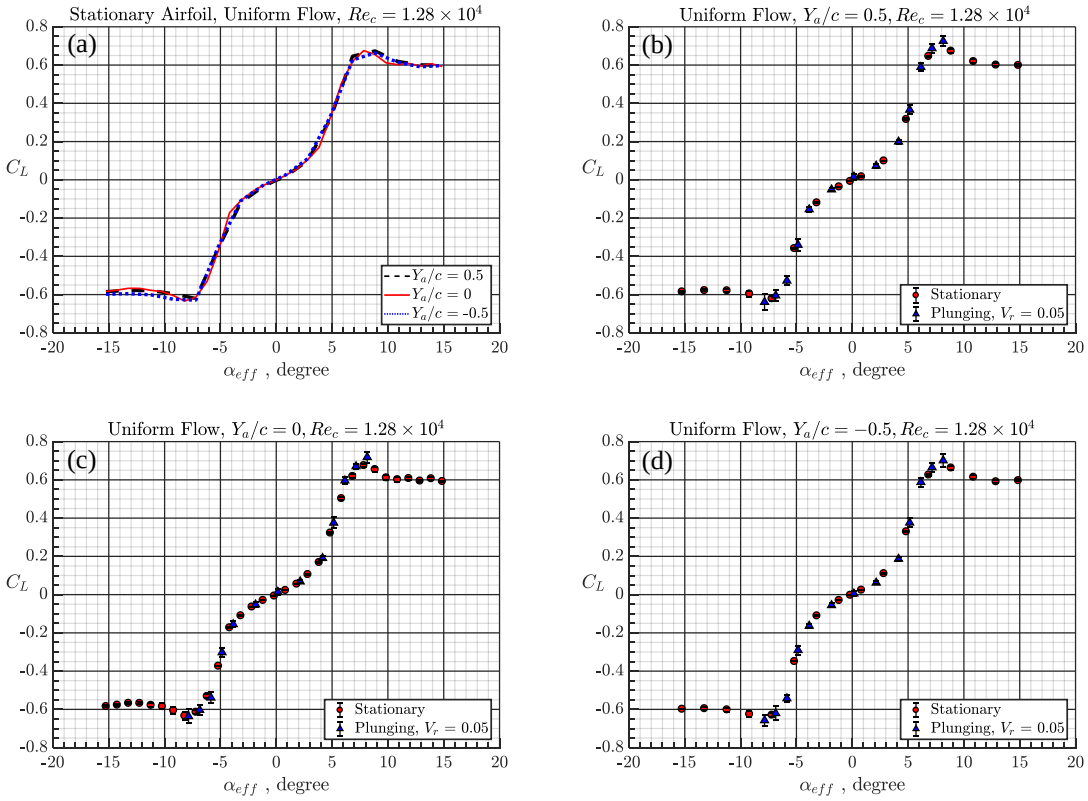

Fig. 7 (a) Stationary airfoil C_L-vs.-α_{eff} curves at the three different cross-stream measurement positions at Re_c = 1.28×10⁴ in uniform flow. Comparison of the stationary and the plunging airfoil C_L-vs.-α_{eff} measurements at (b) Y_a/c = 0.5, (c) Y_a/c = 0, and (d) Y_a/c = -0.5, where Re = 1.28×10⁴ and V_r = 0.05 for the plunging airfoil.

B. Shear Flow Results

Figures 8 and 9 display the C_L-vs.-α_{eff} characteristics of the stationary and the moving airfoils at the three cross-stream measurement positions when shear is present in the approach stream, with corresponding flow parameters given in Table 1. The stationary airfoil exhibits the same general lift curve trend as in Ref. [3], including the negative C_L at zero AoA. A Re_c and/or K effect is observed between the three positions, as the maximum C_L decreases with decreasing Re_c and increasing K, caused by the decrease in approach stream velocity scale u_0. Stall is not observed at Y_a/c = -0.5, where Re_c = 1.00×10⁴ and K = 0.66, compared to the other two positions. The C_L on the moving and the stationary airfoils agree well for $|\alpha_{eff}| \leq 5°$, indicating that the quasi-steady analysis in the Galilean reference frame holds in this AoA and V_r×K range. This allows for approximation of the C_L on a translating airfoil using the C_L on a stationary airfoil at the same α_{eff}. For α_{eff} < -5°, the C_L on the plunging airfoil is still well approximated by that on the stationary airfoil, though some deviation is observed at Re_c = 1.00×10⁴. However, this is in stark contrast to α_{eff} > 5° where the C_L on the translating airfoil becomes larger than the C_L on the stationary airfoil at the same AoA for each position. This deviation grows larger as Re_c decreases and V_r×K increases. The increasing deviation is mostly associated with the decrease in maximum C_L on the stationary airfoil. The airfoil appears to be moving too fast to adapt to the local stationary airfoil C_L-vs.-α_{eff} characteristics at high-positive AoA.

Surprisingly, the plunging airfoil maximum C_L does not appreciably change as Re_c decreases and V_r×K increases. However, the α_{eff} at which maximum C_L occurs varies by about 2° across the cross-stream measurement positions, though this is within the AoA resolution. The most noticeable difference between the plunging airfoil cases is the change of slope of each respective C_L-vs.-α_{eff} curve approaching the maximum C_L point. The slope is approximately the same for each C_L-vs.-α_{eff} curve for 0° < α_{eff} < 2°, then the curves for Y_a/c = 0.5, 0 and -0.5 abruptly change from the original slope at approximately α_{eff} = 2°, 4°, and 6°, respectively. This change of the C_L-vs.-α_{eff} curve slope prior to reaching maximum C_L is essentially delayed by decreasing Re_c and/or increasing V_r×K. Overall, the

results show that the motion across shear produces a fundamental change in the stall behavior of the airfoil versus a stationary airfoil.

Table 1 Flow parameters at the cross-stream measurement positions for the plunging airfoil in shear.

Y_a/c	$u_0\ (cm/s)$	Re_c	V_r	K	$V_r \times K$
0.5	12.4	1.61×10^4	0.040	0.40	0.016
0	10.1	1.31×10^4	0.050	0.50	0.025
−0.5	7.6	1.00×10^4	0.066	0.66	0.044

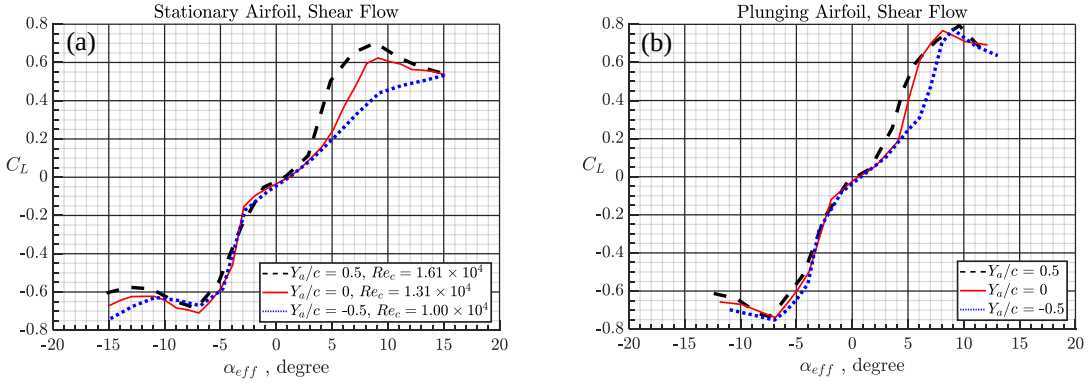

Fig. 8 (a) Stationary airfoil (b) plunging airfoil C_L-vs.-α_{eff} curves at the three different cross-stream measurement positions in shear flow. Refer to Table 1 for the plunging airfoil flow parameters.

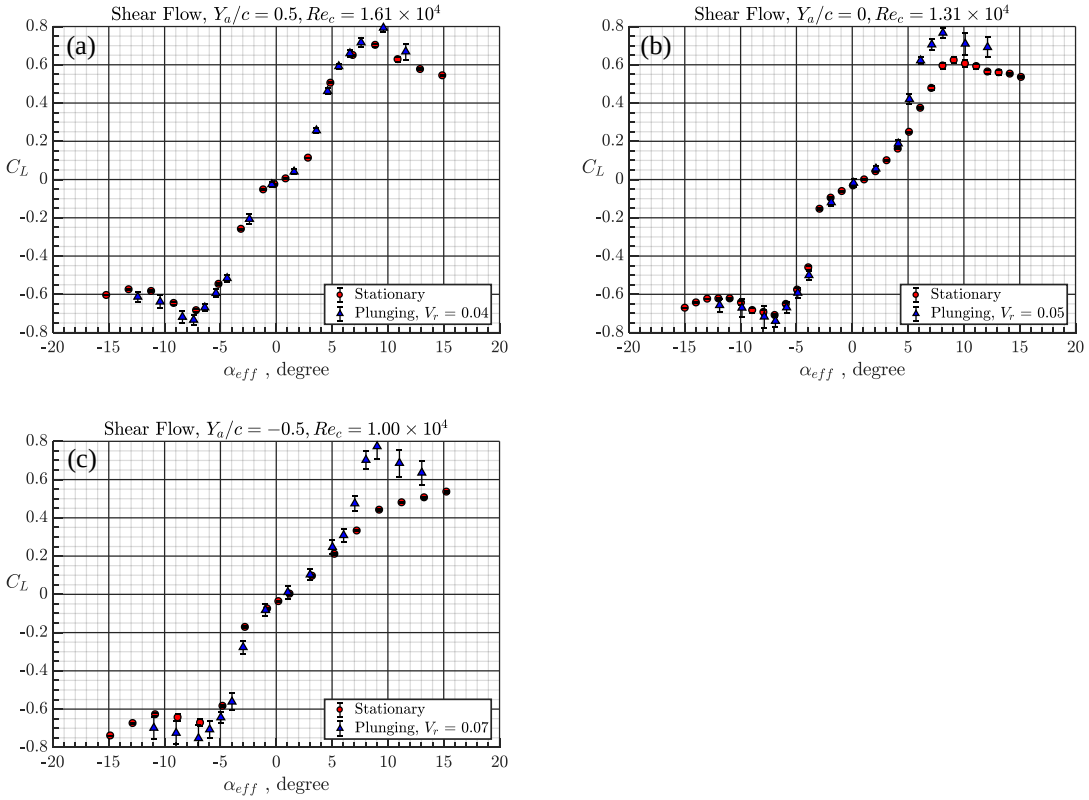

Fig. 9 Comparison of the stationary and the plunging airfoil C_L-vs.-α_{eff} measurements at cross-stream measurement positions (a) Y_a/c = 0.5, (b) Y_a/c = 0, and (c) Y_a/c = -0.5.

IV. Conclusions

The results given herein demonstrate that steady transverse motion of an airfoil across a uniform-shear zone causes significant, fundamental changes in the near-stall and stall C_L characteristics, compared to a stationary airfoil. At lower angles of attack, $|\alpha_{eff}| \leq 5°$, the C_L characteristics are the same for the moving (in a Galilean frame of reference) and the stationary airfoil for the conditions investigated here. A practical implication of this finding is that, within this low-AoA range, lift measurements on a stationary airfoil model in shear flow can be used to obtain the lift characteristics of the moving airfoil under the same flow conditions. A similar conclusion is drawn for negative angles of attack, where the lift coefficients also agree between the stationary and moving airfoils; however, this agreement becomes less precise approaching stall when the Reynolds number is low and the non-dimensional unsteadiness parameter is high. By contrast, the C_L on the moving airfoil at positive angles of attack approaching stall in a Galilean frame of reference cannot be approximated by the stationary airfoil C_L. The difference between these lift coefficients grows with decreasing Re_c and increasing $V_r{\times}K$, which is mostly a reflection of the decreased C_L on the stationary airfoil and simultaneous decreased lift curve slope for the moving airfoil. Interestingly, the maximum C_L on the moving airfoil at each Re_c and $V_r{\times}K$ combination investigated remains effectively unchanged, while the α_{eff} where maximum C_L occurs varies slightly. However, a significant difference between the moving airfoil cases is observed where the slope of the C_L-vs.-α_{eff} curve abruptly changes at different α_{eff} as Re_c decreases and $V_r{\times}K$ increases, after each case starts with the same slope within $0° < \alpha_{eff} < 2°$.

Future investigation is required to fully understand the effect of Re_c, V_r, and K on the force on the plunging airfoil in shear flow. Flow characterization using MTV will be used to investigate the flow over the surface, and in the wake of, the airfoil at several cross-stream positions and angles of attack. This will give insight into how the flow field is affected by the airfoil motion in the presence of uniform shear. The flow field measurements would be compared at both low α_{eff}, where lift agreement is found between the stationary and moving airfoils, and near-stall α_{eff}, where a fundamental change in behavior is observed.

Acknowledgments

This work is supported by Office of Naval Research (ONR) grant number N00014-16-1-2760, and the NDSEG Fellowship Program with ONR as the sponsoring agency. The authors thank Dr. David Olson for his assistance with some of the experiments and data processing. The views and conclusions contained in this document are those of the authors and should not be interpreted as representing the official policies, either expressed or implied, of ONR or the U.S. Government. The U.S. Government is authorized to reproduce and distribute reprints for Government purposes notwithstanding any copyright notation herein.

References

[1] Hammer, P. R., Visbal, M. R., Naguib, A. M., and Koochesfahani, M. M., "Lift on a Steady 2-D Symmetric Airfoil in a Viscous Uniform Shear Flow." *Journal of Fluid Mechanics*, Vol. 837, R2, 2018 (https://doi.org/10.1017/jfm.2017.895)

[2] Tsien, H.-S. "Symmetrical Joukowsky airfoils in shear flow." *Quarterly of Applied Mathematics*, Vol. 1, No. 2, 1943, 130–148.

[3] Hammer, P. R., Olson, D. A., Visbal, M. R., Naguib, A. M., and Koochesfahani, M. M. "An Investigation of the Aerodynamics of a Harmonically-Pitching Airfoil in Uniform-Shear Approach Flow." 2018 AIAA Aerospace Sciences Meeting, AIAA SciTech Forum, (AIAA 2018-0575). (https://doi.org/10.2514/6.2018-0575)

[4] Hamedani, B. A., Naguib, A. M., and Koochesfahani, M. M., "Reynolds Number Effect on Lift Characteristics of an Airfoil Translating Across a Non-uniform Approach Flow." 2019 AIAA Aerospace Sciences Meeting, AIAA SciTech Forum

[5] Gendrich, C. P., Koochesfahani, M. M., and Nocera, D. G. "Molecular tagging velocimetry and other novel applications of a new phosphorescent supramolecule." *Experiments in Fluids*, 23:675–691, 1997. (https://doi.org/10.1007/s003480050123)

[6] Koochesfahani, M. M., and Nocera, D. G. "Molecular tagging velocimetry." In: Tropea, C., Yarin, A. L., Foss, J. F. (eds) *Handbook of Experimental Fluid Dynamics*, Chap 5. Springer, Berlin Heidelberg, 2007, pp 362–382.

[7] Gendrich, C. P., and Koochesfahani, M. M. "A spatial correlation technique for estimating velocity fields using molecular tagging velocimetry (MTV)." *Experiments in Fluids*, 22(1), 1996, 67-77. (https://doi.org/10.1007/BF01893307)

[8] Kotansky, D. R. "The use of honeycomb for shear flow generation." *AIAA Journal*, Vol. 4, No. 8, 1966, pp. 1490-1491. (https://doi.org/10.2514/3.3724)

[9] Safaripour, A., Olson, D., Naguib, A., and Koochesfahani, M. "On Using Shaped Honeycombs for Experimental Generation of Arbitrary Velocity Profiles in Test Facilities." *Bulletin of American Physical Society*. Vol. 61, No. 20, 2016, p. 265.